Cholesterol enhances surface water diffusion of phospholipid bilayers

Chi-Yuan Cheng,[1,a)] Luuk L. C. Olijve,[2,a)] Ravinath Kausik,[1,b)] and Songi Han[1,c)]
[1]*Department of Chemistry and Biochemistry and Materials Research Laboratory, University of California, Santa Barbara, California 93106, USA*
[2]*Laboratory of Macromolecular and Organic Chemistry and Institute for Complex Molecular Systems, Eindhoven University of Technology, P.O. Box 513, 5600 MB, Eindhoven, The Netherlands*

(Received 29 July 2014; accepted 29 September 2014; published online 17 October 2014)

Elucidating the physical effect of cholesterol (Chol) on biological membranes is necessary towards rationalizing their structural and functional role in cell membranes. One of the debated questions is the role of hydration water in Chol-embedding lipid membranes, for which only little direct experimental data are available. Here, we study the hydration dynamics in a series of Chol-rich and depleted bilayer systems using an approach termed ^{1}H Overhauser dynamic nuclear polarization (ODNP) NMR relaxometry that enables the sensitive and selective determination of water diffusion within 5–10 Å of a nitroxide-based spin label, positioned off the surface of the polar headgroups or within the nonpolar core of lipid membranes. The Chol-rich membrane systems were prepared from mixtures of Chol, dipalmitoyl phosphatidylcholine and/or dioctadecyl phosphatidylcholine lipid that are known to form liquid-ordered, raft-like, domains. Our data reveal that the translational diffusion of local water on the surface and within the hydrocarbon volume of the bilayer is significantly altered, but in opposite directions: accelerated on the membrane surface and dramatically slowed in the bilayer interior with increasing Chol content. Electron paramagnetic resonance (EPR) lineshape analysis shows looser packing of lipid headgroups and concurrently tighter packing in the bilayer core with increasing Chol content, with the effects peaking at lipid compositions reported to form lipid rafts. The complementary capability of ODNP and EPR to site-specifically probe the hydration dynamics and lipid ordering in lipid membrane systems extends the current understanding of how Chol may regulate biological processes. One possible role of Chol is the facilitation of interactions between biological constituents and the lipid membrane through the weakening or disruption of strong hydrogen-bond networks of the surface hydration layers that otherwise exert stronger repulsive forces, as reflected in faster surface water diffusivity. Another is the concurrent tightening of lipid packing that reduces passive, possibly unwanted, diffusion of ions and water across the bilayer.
 [http://dx.doi.org/10.1063/1.4897539]

I. INTRODUCTION

Hydration water in the vicinity of biomolecular surfaces is thought to play a crucial role in mediating the structural organization of biological constituents and their functions.[1–4] For example, water drives the self-assembly of lipid bilayers,[1] while water may actively modulate ligand binding or recognition events of proteins by forming or breaking hydrogen bonds at the binding interface.[2–4] The diffusion dynamics of water molecules associated with the protein or lipid membrane surface entails hydrogen-bond rearrangement of the liquids.[4] Consequently, faster (slower) diffusivity of hydration water reflects on lower (higher) energy barrier for the formation and breaking of hydrogen bonds between water molecules in close proximity to the biomolecular surfaces, encompassing up to at least 2–3 hydration layers off the surface.[5–7] Rapid hydrogen-bond rearrangements and fast water diffusivity near the protein-water interface are suggested to be critical to protein folding, protein-protein or protein-ligand interactions.[8,9] In cell membranes, cholesterol (Chol) plays a key role in regulating the structure and function of membrane proteins and biological membranes. Chol at a biological-relevant concentration of 20–30 mol.% promotes the activation of membrane proteins, apparently by reducing the free energy barrier for transferring a protein from an inactive to an active state.[10] In fact, at 20–30 mol.% Chol concentrations, ternary mixtures of saturated and unsaturated lipids together with Chol are known to segregate into coexisting nanoscale lipid domains within biological membranes, also known as lipid rafts, that act as platforms for signal transduction and cell adhesion.[11,12] Membrane proteins appear to be better solubilized in Chol-containing membranes, enhancing their yield, concentration, stability, as well as activity and function.[13,14]

It has been proposed that Chol modulates membrane protein function by directly stabilizing the structure of the membrane protein[15] or by indirectly altering the hydration or packing of the lipid bilayers.[11] In either case, water is intimately involved in these processes at the protein-lipid interfaces, e.g., by strengthening hydrogen bonds between water and the membrane constituents or by modulating water content in the

[a)]Chi-Yuan Cheng and Luuk L. C. Olijve contributed equally to this work.
[b)]Present address: Schlumberger Doll research, Cambridge, Massachusetts 02139, USA.
[c)]Author to whom correspondence should be addressed. Electronic mail: songi@chem.ucsb.edu

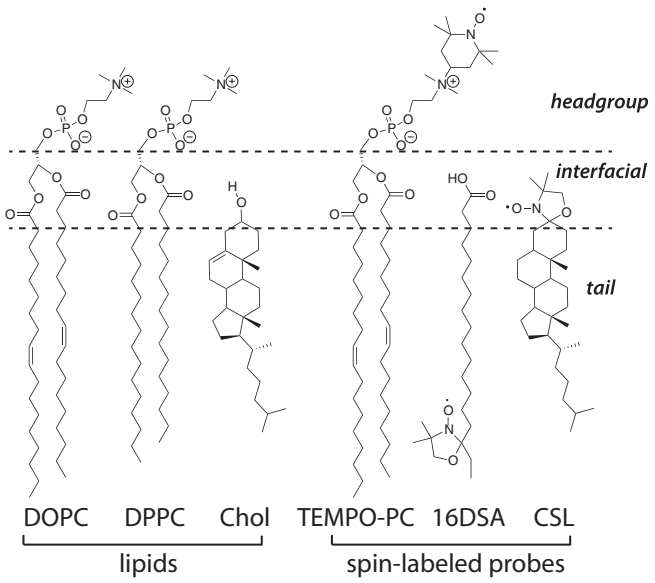

CHART 1. Structures of lipids and spin-labeled probes used in this study.

bilayer.[16–18] For instance, the activity of Na^+/K^+-ATPase in native membranes has been reported to strongly correlate with Chol and water content, with the maximal activity found at 30 mol.% Chol,[19] where the maximal water content at the protein-lipid interface was observed.[17–19] In lipid membrane systems without embedded proteins; however, water content within the bilayer decreases in the presence of Chol, as evidenced by electron paramagnetic resonance (EPR)[20,21] and fluorescence anisotropy measurements.[16,17] Although extensive research has been performed in model cell membranes to characterize the Chol-containing lipid mixtures at various lipid phases and compositions,[21–36] the molecular basis underlying the biological effect of Chol in lipid-water assemblies remains unclear.

Chol is an amphiphilic molecule that inserts into a bilayer with its hydroxyl group pointed towards the bilayer surface and the long molecular axis oriented nearly parallel to the bilayer normal.[30,37] The chemical structure of Chol and its relative position to the phosphatidyl choline (PC) lipids is illustrated in Chart 1. Several lines of evidence suggest that Chol increases the molecular ordering of the PC acyl chain[30–36] and enhances the lipid packing in the membrane (i.e., condensation effect),[38] resulting in a decreased area per lipid concurrent with a substantial bilayer thickening.[24,39,40] This condensation effect is more pronounced in saturated PC lipids than in unsaturated PCs.[41] Clearly, the lateral condensation effect of lipid bilayers induced by Chol can rationalize the reduced permeability of small solutes (e.g., ions or amino acids) and water across the bilayer.[20,42–45] Moreover, this condensation effect yields a new thermodynamic phase on a macroscopic level, as reflected in the unique fluidity of lipid bilayers. When Chol concentration is sufficiently high, a liquid-ordered phase (l_o) can be observed, whose property is distinct from the tightly packed solid-ordered phase (s_o, also known as gel phase, g) and fluid liquid-disordered phases (l_d, also known as liquid-crystalline phase, L_α), both of which are well-known in the single-component PC bilayer systems.[31–36] This new l_o phase is peculiar as it exhibits a high degree of structural ordering of the acyl chains resembling the gel phase, while the lipids diffuse at a rate comparable to those found in the fluid phase.[41] At intermediate Chol concentration, membranes can undergo a lipid-lipid phase separation between l_d and l_o phases,[31–36] as has been observed in binary (saturated-PC/Chol) and ternary lipid mixtures (saturated-PC/unsaturated-PC/Chol).[31–36] Crucially, the phase behavior of ternary lipid mixtures is considered to be a robust and simple model for a biological membrane, because their phase diagrams are known[31–36] and because they can reproduce key properties associated with rafts in cell membranes.[46,47] Recent studies suggest that binary lipid mixtures exhibit local phase separation at the nanometer length scale with global homogeneities,[46,48–50] whereas ternary lipid mixtures seem necessary to obtain lateral phase separation between lipid phases with larger-scale spatial heterogeneities.[46,51] Despite these existing models, the nature of Chol-lipid interactions, and how the lipid-lipid phase separation contributes to lateral heterogeneity of membranes and lipid raft formation are still subjects of debate.[11]

The landscape of surface hydration dynamics of biomolecular complexes and its relationship to biological functions has long been the subjects of intense interest for both experimentalists and theorists;[52–55] however, theoretical studies are by far ahead of experimental access to parameters of interest.[56–58] Despite an overwhelming interest in understanding the role of hydration dynamics in lipid membrane biophysics, direct experimental observation has proven challenging, given the lack of tools to distinguish the few layers of hydration water interacting with the biological systems from the bulk water under ambient conditions. In this study, we investigate the role of Chol in modulating the surface and interior hydration dynamics in synthetic lipid bilayer systems, and discuss its potential implication to the membrane biophysics. We exploit Overhauser dynamic nuclear polarization (ODNP) relaxometry[59–61] and continuous wave (cw) EPR spectroscopy to measure the site-specific hydration dynamics and lipid structural ordering in Chol-containing lipid bilayers, respectively. ODNP measures translational diffusivity of water molecules interacting with site-specific nitroxide radical-based spin labels, tethered either on the surface or within the bilayer of the model lipid membrane systems, with the motional timescale of water between several picosecond (ps) and sub-nanosecond (ns).[59–61] The coupling between the spin labels and water is exclusively modulated by the time-dependent dipolar relaxation between the unpaired electron spin of the label and the water protons at 0.35 T, resulting in the sensitive detection of translational diffusivity of local water within 5–10 Å distance of the spin labels. Our studies reveal that Chol enhances the mobility of lipid headgroups, as well as accelerates the diffusivity of surface water near the lipid membrane surface. Contrary, it impedes the lipid mobility and water diffusivity within the bilayers. The consequently altered hydration dynamics landscape in lipid bilayers upon Chol addition sheds light on the role of Chol and Chol-rich lipid rafts in altering and modulating the mode of interaction between biological constituents and the lipid membrane platform.

II. THEORY

A. Overhauser dynamic nuclear polarization

ODNP relies on the polarization transfer from the electron spins of the nitroxide radicals to the ^{1}H nuclei of the locally interacting water molecules through dipolar interaction.[62] The time-dependent mathematical description of ODNP in liquids is

$$\frac{dI_z}{dt} = -\left(\rho + T_{10}^{-1}\right)(I_z - I_0) - \sigma(S_z - S_0), \tag{1}$$

where I and S refer to nuclear and electron spins, I_0 and S_0 are their Boltzmann equilibrium values, T_{10}^{-1} is the nuclear spin relaxation rate resulting from all other mechanism not to paramagnetic relaxation. The self-relaxation rate and cross-relaxation rate are defined as $\rho = w_0 + 2w_1 + w_2$ and $\sigma = w_2 - w_0$, respectively, where w_0, w_1, and w_2 are nuclear-electron zero-, single-, and double-quantum transition rates. The steady-state solution of Eq. (1) under continuous microwave (MW) irradiation at the allowed electron spin transition frequency leads to the NMR signal enhancement

$$\begin{aligned} E &= \frac{\langle I_z \rangle}{I_0} = 1 - \xi f s \left|\frac{\gamma_e}{\gamma_H}\right| \\ &= 1 - \left(\frac{w_2 - w_0}{w_0 + 2w_1 + w_2}\right)\left(\frac{w_0 + 2w_1 + w_2}{w_0 + 2w_1 + w_2 + T_{10}^{-1}}\right) s \left|\frac{\gamma_e}{\gamma_H}\right|, \end{aligned} \tag{2}$$

where ξ is the coupling factor, f is the leakage factor, s is the saturation factor, and γ_e and γ_H are the gyromagnetic ratios of the electron and ^{1}H, given $|\gamma_e/\gamma_H| = 658$. Ideally, s is approaching 1 for a fully saturated electron spin transition. The coupling factor ξ describes the efficiency of cross-relaxation between the electron and ^{1}H spins, which is defined by $\xi = \sigma/\rho$. The coupling factor carries the information of the relative dynamics between the ^{1}H spins of water and the electron spins of the nitroxide radical, and is therefore the quantity of interest. The leakage factor f accounts for the nuclear spin lattice relaxation originating from the interaction with electron spins compared to all other contributing mechanisms, yielding $f = 1 - T_1/T_{10}$, where T_1 and T_{10} are the ^{1}H longitudinal relaxation time in the presence and absence of the radical, respectively. By extrapolating to infinite MW power, the maximal signal enhancement E_{max} can be determined. The saturation factor s can be extrapolated to maximal saturation $s_{max} \approx 1$,[59,60] which is a valid approximation for slow tumbling macromolecules or assemblies, such as proteins or lipid vesicles studied here.[59,60,63] The coupling factor can then be determined from Eq. (2). It is noted that ξ is field dependent. Here, we study the hydration dynamics in lipid membrane systems using ODNP at a magnetic field of 0.35 T, yielding a Larmor frequency for the electron spin of $\omega_e = 9.8$ GHz and for the ^{1}H spin of $\omega_H = 14.8$ MHz. For small molecules in solution, an extreme motional narrowing regime is approached at 0.35 T, yielding $\omega_H\tau \ll \omega_e\tau \ll 1$, where τ is the translational correlation time of the solvent molecules in solution (i.e., we focus on water here). Thus, the coupling factor at this field is modulated by the molecular dynamics of water dipolar coupled with the spin label, whose motional modes on the order of ω_e. In this regime, the closer the correlation time τ of water with respect to the spin label nearby is to 100 ps ($\approx 1/\omega_e$), the more effectively will it modulate the coupling factor. Therefore, ODNP at 0.35 T is extremely sensitive to motion dictated by the translation correlation time τ of water on the tens of up to 1000 ps timescale, covering a wide motional range of water in hydrated macromolecules and soft matter, from the weakly coupled water on the biological surfaces to deeply buried sites in the core of biomacromolecules or their assemblies.[5–7,61,64–70]

In order to quantify the τ value from ξ, the appropriate model governing the dynamic parameters of the solvent molecules interacting with the spin labels has to be applied. For nitroxide radicals free in water, as well as nitroxide radicals tethered on the surface of liposomes, the force-free hard-sphere model[71] has been shown to give a good fit to field cycling relaxometry data[72–75] and can be used to model the spectral density function. This method becomes especially convenient, when translation diffusion is the dominant modulator of the electron spin-mediated nuclear spin relaxation that is driven via dipolar coupling between the electron and ^{1}H nuclear spins. This model can be employed in our systems as freely diffusing water interacts with the radicals incorporated on the surface and in the bilayer interior of lipid vesicles.[5,65–67] In this case, the coupling factor is given by

$$\xi = \frac{6J(\omega_e + \omega_H, \tau) - J(\omega_e - \omega_H, \tau)}{6J(\omega_e + \omega_H, \tau) + 3J(\omega_H, \tau) + J(\omega_e - \omega_H, \tau)} \tag{3}$$

with following spectral density function:[71]

$$J(\omega, \tau) = \frac{8\tau}{27b^3} \frac{1 + \frac{5\sqrt{2}}{8}(\omega\tau)^2 + \frac{1}{4}\omega\tau}{1 + (2\omega\tau)^{1/2} + \omega\tau + \frac{\sqrt{2}}{3}(\omega\tau)^{3/2} + \frac{16}{81}(\omega\tau)^2 + \frac{4\sqrt{2}}{81}(\omega\tau)^{5/2} + \frac{1}{81}(\omega\tau)^3}, \tag{4}$$

where b is the distance of the closest approaches between electron and ^{1}H spins. Equations (3) and (4) enable the determination of the τ value, which is inversely proportional to local water diffusivity (i.e., $\tau \propto D^{-1}$). In order to compare water diffusivity in different local environments, we introduce the retardation factor, τ/τ_{bulk}, which is the ratio of the τ value of hydration water to that of bulk water, τ_{bulk}. The retardation factor is typically 2–5 for hydration water on water-exposed surfaces of protein or lipid membrane,[6,57,68,75,76] whereas it is around 5–11 in the bilayer interior of lipid assemblies.[72,77,78] However, the relatively modest retardation factor for water within the lipid bilayer only reports on the relatively fast

diffusion dynamics of the highly sparse water molecules across the bilayer, but does not provide any information about water content.[67] It is necessary to clarify that we assume a full exchange of water molecules between hydration layer and bulk water within the timescale of ODNP build-up time that is on the order of the T_1 of water protons (i.e., few seconds),[61] so that no pool of unenhanced bulk water skews the ODNP-derived local hydration dynamics. The timescale for the exchangeable protons between water molecules and lipid bilayer surface around the nitroxide radicals is on the order of milliseconds to sub-seconds,[79] so that a full exchange between the surface and bulk water populations is ensured,[79] while it is too long to directly influence the timescales of water diffusion at tens to hundreds of ps derived by ODNP at 0.35 T. Therefore, the exchangeable protons should have no influence on our ODNP results.

In addition to the standard analysis of ξ, we can separately determine local water mobility at fast timescale (ps) and at slow timescale (ns) using the relaxivity at the electron and ^{1}H Larmor frequency, respectively.[61,62,69] Typically, the hydration dynamics at several ns or longer timescales is contributed from bound water, whereas hydration dynamics at ps timescale is contributed from loosely bound and freely diffusing water at or near molecular interfaces. This analysis is model-independent and permits the direct comparison of different classes of hydration waters in different local environments. However, it does not easily yield an explicit value for τ as with the standard analysis. k_σ is the cross-relaxivity between electron and ^{1}H spins driven by electron spin-flip excitation at ω_e at a known spin-labeled concentration C_{SL},

$$k_\sigma = \frac{1 - E_{max}}{C_{SL} T_1} \left| \frac{\gamma_H}{\gamma_e} \right|. \tag{5}$$

Therefore, k_σ is exclusively sensitive to characteristics of fast water diffusion of loosely bound water at tens of ps to sub-ns timescale. On the other hands, k_ρ is the self-relaxivity, which represents the paramagnetic contributions to T_1 relaxation rates of water driven by dipolar self-relaxation of water protons,

$$k_\rho = \frac{T_1^{-1} - T_{10}^{-1}}{C_{SL}}. \tag{6}$$

Both k_σ and k_ρ relaxivities probe the values of the spectral density function for fluctuations in dipolar relaxation between electron and ^{1}H. Since $\omega_H \ll \omega_e$, the relaxivities can be approximated as follows:

$$k_\sigma = 6J(\omega_e + \omega_H, \tau) - J(\omega_e - \omega_H, \tau) \approx 5J(\omega_e, \tau), \tag{7}$$

$$\begin{aligned} k_\rho &= 6J(\omega_e + \omega_H, \tau) + 3J(\omega_H, \tau) + J(\omega_e - \omega_H, \tau) \\ &\approx 7J(\omega_e, \tau) + 3J(\omega_H, \tau). \end{aligned} \tag{8}$$

The coupling factor can then be approximated

$$\xi = \frac{\sigma}{\rho} = \frac{C_{SL} k_\sigma}{C_{SL} k_\rho} \approx \frac{5J(\omega_e, \tau)}{7J(\omega_e, \tau) + 3J(\omega_H, \tau)}. \tag{9}$$

To extract the relaxivity that only depends on the value of the spectral density function for fluctuations of dipolar relaxation at ω_H, the contribution from fast waters (k_σ) can be subtracted from the self-relaxivity (k_ρ) as follows,[61] based on Eqs. (7) and (8):

$$k_{low} \approx \frac{5}{3} k_\rho - \frac{7}{3} k_\sigma \approx 5J(\omega_H, \tau), \tag{10}$$

which is strongly weighted by bound water at slower motion timescale (few ns). Thus, the contribution of slow or bound water diffusing at slower timescale (i.e., $1/\omega_H \sim 6.7$ ns at 0.35 T) can be determined by k_{low}. Recent hardware developments for ODNP have further improved the reliability for quantifying local surface hydration dynamics at 0.35 T. The reproducibility of the ODNP data are presented in Table S1 of the supplementary material.[80] Importantly, the error from variations between repeat experiments is larger than the fitting error derived from data within a given experimental run, which provides an upper bound. Therefore, we reported the experimental errors (e.g., in Figs. 2–4) from repeat measurements in this study. ODNP at different magnetic field strength, i.e., at different MW frequencies, will be an important future perspective as different motional timescales associated with different MW frequencies can be probed. However, these future attempts require substantial hardware and method developments. In this work, we focus on ODNP measurements at 0.35 T and 9.8 GHz MW frequency that represents an ideal timescale to probe the translational dynamics of hydration water moving with correlation times on the order of few ps to sub-ns.

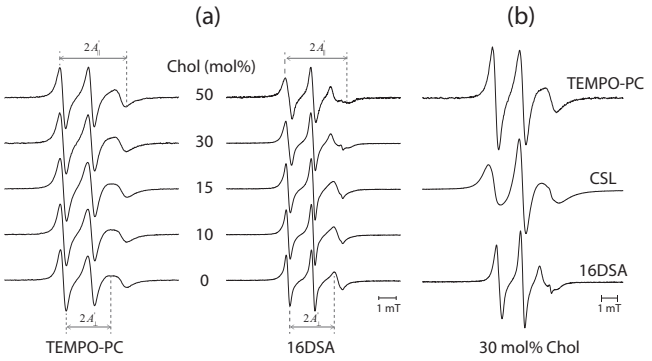

FIG. 1. (a) Representative cw EPR spectra using TEMPO-PC and 16DSA in DOPC/DPPC/Chol bilayer systems at various cholesterol (Chol) concentrations. (b) EPR spectra using TEMPO-PC, CSL, and 16DSA in the DOPC/DPPC/Chol (3.5:3.5:3 mol:mol:mol%) bilayer system.

B. Order parameter deduced by EPR spectral analysis

The molecular order parameter S can be obtained from EPR spectral analysis of nitroxide spin-labeled probes in lipid bilayers. The order parameter is related to the angular amplitudes of the motion of the nitroxide radical, which reflects the packing or ordering of the acyl chain or headgroup of PC lipid molecules, to which the spin label is tethered.[81] The order parameter of a rod-like spin-labeled probe in a lipid bilayer is given by $S \equiv \langle \frac{1}{2}(3\cos^2\theta - 1) \rangle$, where θ is the angle between the long molecular axis of the spin-labeled lipid and bilayer normal, and the bracket denotes the average taken over the orientation distribution and time. The direction of the z-vector

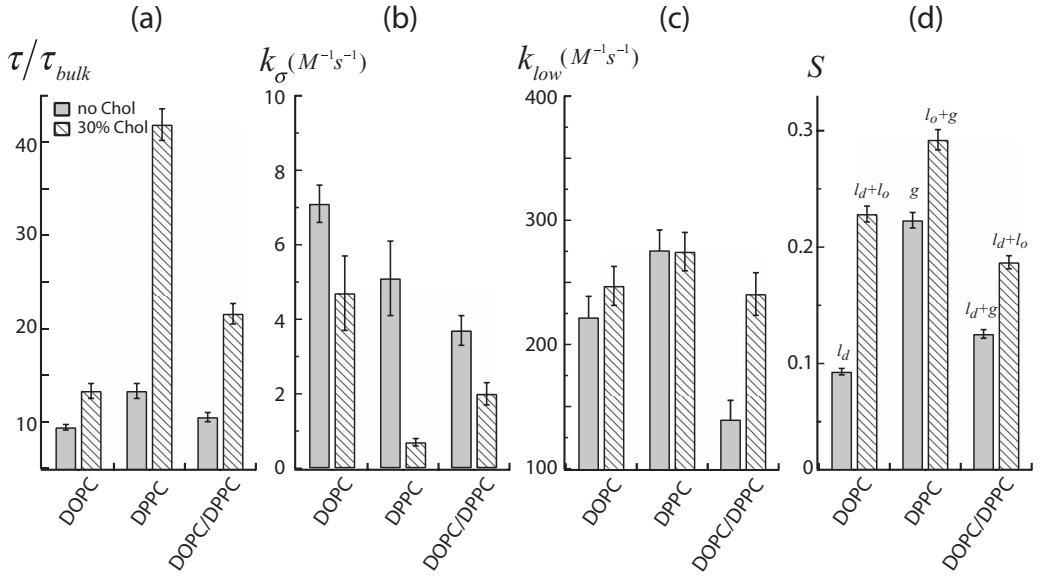

FIG. 2. Hydration dynamics of bilayer-internal water deducted by (a) τ/τ_{bulk} (b) k_σ (c) k_{low} values and order parameter (S) within lipid bilayers of DOPC, DPPC, and DOPC/DPPC (1:1, mol:mol.%) (as probed by 16DSA) in the absence and presence of 30 mol.% cholesterol (Chol). Lipid phases for the corresponding lipids are indicated in (d).

of the nitroxide moiety of the 16-doxyl-stearic acid (16DSA) spin label is parallel to the 2pz orbital of the nitrogen atom of the nitroxide and the direction of the x-vector of the nitroxide moiety of 1,2-dioleoyl-*sn*-glycero-3-phospho(tempo)choline (TEMPO-PC) is parallel to the N-O vector of the nitroxide, both corresponding to the long molecular vectors of 16DSA and TEMPO-PC, respectively.[81] The chemical structures of these spin labels and their approximate locations in the lipid bilayer are illustrated in Chart 1. A completely isotropic orientation of nitroxide spin label probes results in $S = 0$. In contrast, when the packing or ordering of the spin-labeled lipid is very tight, θ is close to zero, leading to $S \approx 1$. The positions of cw EPR spectral lines at X band (i.e., 9.8 GHz) in solution, which are determined by the time-average of hyperfine and g-tensor components, are independent of differences in spin label-intrinsic mobility, as long as it is in the extreme narrowing regime, where rotational correlation time of spin-label is $\ll 1/\omega_e$. It is rather determined by the cone of the θ angle, which is restricted as imposed by the lipid membrane environment. In this work, we quantify the order parameter S, as suggested in the work by Hubbell *et al.*:[81]

$$S = \frac{A'_{\parallel} - A'_{\perp}}{A_{zz} - \frac{1}{2}(A_{xx} + A_{yy})}, \tag{11}$$

where $2A'_{\parallel}$ is the outer hyperfine splitting and $2A'_{\perp}$ is inner hyperfine splitting measured in a cw EPR spectrum, where

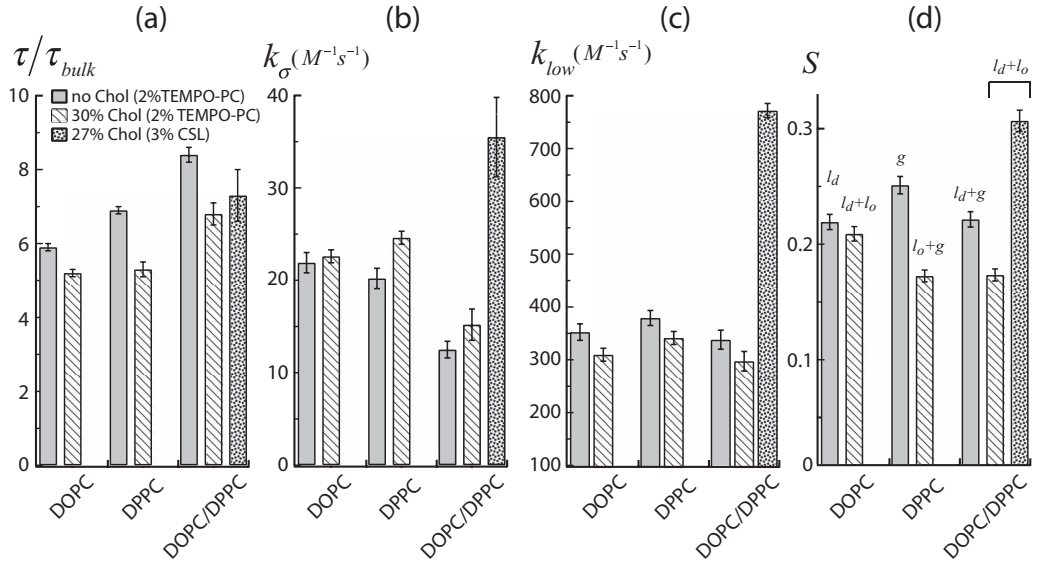

FIG. 3. Hydration dynamics of surface water deducted by (a) τ/τ_{bulk} (b) k_σ (c) k_{low} values and order parameter (S) on the surface of DOPC, DPPC, and DOPC/DPPC (1:1 mol:mol.%) vesicles (as probed by TEMPO-PC or CSL) in the absence and presence of 30 mol.% cholesterol (Chol). Lipid phases for the corresponding lipids are indicated in (d).

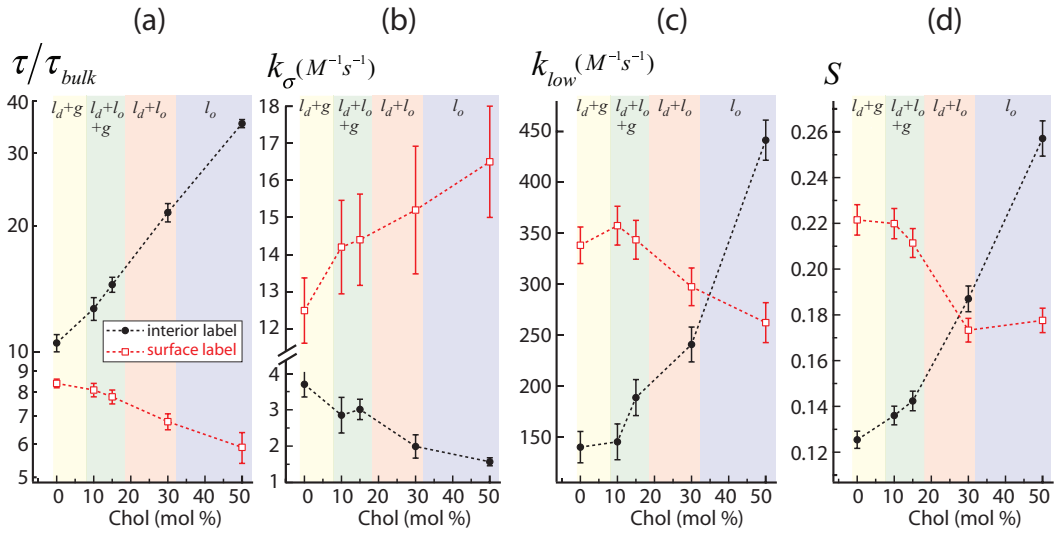

FIG. 4. Hydration dynamics deducted by (a) τ/τ_{bulk}, (b) k_σ, and (c) k_{low} values and order parameter (S) on the surface and interior of DOPC, DPPC, and DOPC/DPPC (1:1, mol:mol.%) vesicles (as probed by TEMPO-PC or 16DSA) at various cholesterol (Chol) concentration. Lipid phases for tertiary mixture at the corresponding Chol concentration are indicated.

A_{xx}, A_{yy}, and A_{zz} are the principal values of the hyperfine coupling tensor. In this study, the order parameters were calculated based on the published values of (A_{xx}, A_{yy}, A_{zz}) = (5.6, 5.6, 34.5) mT as previously determined for TEMPO-PC,[22,23] (32.6, 5.0, 5.0) mT for 16DSA,[22,23] and (34.0, 5.8, 5.8) mT for CSL[22] spin label. The representative cw EPR spectra of DOPC/DPPC/Chol systems are illustrated in Fig. 1.

III. RESULTS

A. Model lipid membrane systems

In this study, we carried out experiments using model liposomal bilayer systems under ambient aqueous solution conditions that maintain key properties of biological membranes. The structures of the lipid molecules used in this work are illustrated in Chart 1. Ternary lipid mixtures composed of unsaturated PCs (e.g., DOPC or POPC), saturated lipids (e.g., sphingomyelin or DPPC), and Chol have been postulated to be robust model systems to mimic cellular membranes.[35,46,47] In these model systems, Chol strongly favors partitioning into the domains rich in saturated PCs rather than into the domains rich in unsaturated PCs.[36] Here, we study the effect of Chol on phospholipid bilayers by systematically partitioning increasing amounts of Chol into three liposome systems: pure DOPC, pure DPPC, and a binary mixture of DOPC/DPPC (1:1 mol:mol.%).[31–36] We investigated Chol concentrations varying from 0 to 50 mol.%, with particular emphasis a biological relevant concentration of 30 mol.% Chol, as Chol at this concentration induces phase separation in the DOPC/DPPC/Chol mixture.[31–36] To obtain a more complete molecular picture of the Chol effect on lipid bilayers than known to date, we quantify a range of spectroscopic parameters that display changes in the local hydration dynamics and lipid ordering, selectively at the lipid bilayer surface and interior in Chol-rich and Chol-free lipid mixtures, in reference to known phase diagrams for Chol-containing lipid bilayer systems.[31–36]

TEMPO-PC and 16DSA are widely used stable nitroxide spin-labeled lipid or surfactant probes, respectively. TEMPO-PC with a nitroxide moiety attached off the choline of the PC headgroup is used to probe hydration dynamics and lipid ordering on the surface of lipid bilayers (see Chart 1). The nitrogen of TEMPO-PC's nitroxide is known to reside 5 Å above the lipid phosphate level, i.e., probes a surface region with minimal lipid and predominant water density.[82] In contrast, 16DSA, which has a nitroxide radical on the 16th carbon of acyl chain of phospholipid, is used for measuring hydration dynamics and lipid ordering within the hydrophobic core of the lipid bilayer.[65–67] To study the hydration dynamics and lipid ordering slightly below the lipid headgroup in the presence and the vicinity of Chol,[23] we employed a nitroxide spin-labeled Chol analogue, 3β-doxyl-5α-cholestane (CSL) (see Chart 1), which has been used to study the dynamics and ordering of Chol in model membranes by cw EPR.[23,24,83] In CSL, the polar 3β-OH headgroup of Chol is replaced by a doxyl group, but still shows the same overall molecular characteristics and rotational diffusion rates as expected for Chol, according to a high-field EPR study.[83] Fig. 1(a) exhibits the cw EPR spectra of TEMPO-PC and 16DSA incorporated in DOPC/DPPC/Chol membrane suspensions recorded at various Chol concentrations. As expected, changes of EPR lineshapes probed by 16DSA (Fig. 1(a)) upon addition of Chol to the lipid membrane reflect increased ordering of the lipid bilayers due to condensation effects. Fig. 1(b) compares the cw EPR spectra of TEMPO-PC, CSL, and 16DSA in DOPC/DPPC/Chol suspensions at the Chol concentration of 30 mol.%. The nitroxide based spin-label probes (TEMPO-PC, 16DSA, or 16PC probes) have been demonstrated to be viable for the study of lipid membrane dynamics and local polarity in various systems by cw EPR,[84,85] as well as paramagnetic relaxation enhancement NMR.[86] The incorporation of spin probes into lipid membrane systems has shown minimal disturbance to the lipid membranes.[87,88] To minimize perturbation to the lipid bilayer, a low concentration of the spin-label probes (2 mol.%) of TEMPO-PC or 16DSA, that

has been verified to not affect lipid packing of DOPC and DPPC by means of leakage experiments[67] was used in this study.

B. Hydration dynamics and lipid ordering in the hydrophobic bilayer interior of liposomes

Fig. 2 depicts ODNP and EPR analysis of lipid vesicles with spin labels located within the bilayer core, on average in the vicinity of the 16th carbon position of the acyl chain using 16DSA, of DOPC, DPPC, and DOPC/DPPC liposome systems with and without the incorporation of 30 mol.% Chol into their bilayers. Although it has been postulated that the nitroxide radical of 16DSA located near the chain terminus may bend back to the aqueous surface,[87] EPR measurements shows that the polarity profile at different depths in l_o and l_d phases can be faithfully characterized by a sigmoidal decay curve,[85] where the asymptotic minimum is reached near the 10th carbon of acyl chains.[85] This finding suggests that 16DSA is still valid for probing, on average, the intrinsic local water environment in the bilayer center. In lipid bilayer systems depleted of Chol, we find that local translational diffusivity of hydration water within the DPPC bilayer is 1.4 fold slower than within the DOPC bilayer (Fig. 2(a)), reflecting the expected tighter packing of the DPPC (g phase) than the DOPC (l_d phase) bilayer. This result agrees with previous findings that water permeability across saturated-PC bilayer is about 1.4–4.2 fold slower than across unsaturated-PC bilayers.[45,89] Interestingly, τ/τ_{bulk} of the bilayer-internal water in DOPC/DPPC liposomes, which is well-established to coexist in the $l_d + g$ phase,[32] is between the τ/τ_{bulk} values found in the l_d and g phase bilayers. Upon incorporating 30 mol.% Chol into pure DOPC or DPPC bilayers, the water diffusivity within the lipid bilayers of either membrane system clearly exhibits a significant retardation, as reflected in an increasing τ/τ_{bulk} value from 9.4 to 13.3 for DOPC and from 13.3 to 41.9 for DPPC. This finding is consistent with early observations that Chol impedes water permeability within lipid bilayers.[20,44,45] We further analyzed ODNP data by separately evaluating k_σ and k_{low} values that depict the motion of local water at different timescales, as presented in Figs. 2(b) and 2(c). We found that the trend of k_σ is quantitatively anti-correlated to the trend of k_{low} when 30 mol.% Chol is added to lipid bilayer membranes made of pure DOPC, pure DPPC, as well as DOPC/DPPC mixtures, confirming that k_σ and k_{low} of bilayer-internal water is contributed from different motional timescales of water, once the l_o phase forms. Specifically, an incorporation of 30 mol.% Chol reduces k_σ of bilayer-internal water in DOPC, DPPC, and DOPC/DPPC systems (Fig. 2(b)), whereas it increases k_{low} in all three lipid mixtures (Fig. 2(c)). This result suggests that the presence of 30 mol.% Chol leads to more bound water and the freely moving water to diffuse more slowly within the bilayers of DOPC, DPPC, and DOPC/DPPC systems.

Fig. 2(d) illustrates the order parameter S of the nitroxide radical of 16DSA within the bilayer of DOPC, DPPC, and DOPC/DPPC mixtures. The order parameter profile of 16DSA-labeled lipid bilayers without Chol shows differences between the l_d, g, and the coexisting $l_d + g$ phases, following DPPC (g) > DOPC/DPPC ($l_d + g$) > DOPC (l_d). As expected, the comparative trend for the order parameter persists but shows significantly more ordering in the presence of 30 mol.% Chol in all three systems due to the condensation effect.[38] These results are in excellent quantitative agreement with previous EPR studies.[22,90] Importantly, in the DPPC bilayer systems, although the S value shows a 31% increase upon addition of 30 mol.% Chol, the τ/τ_{bulk} value for the bilayer-internal water demonstrates a much greater retardation (>200%) when 30 mol.% Chol is added. This observation implies that the retardation of the bilayer-internal water is not simply proportional to the Chol-induced physical confinement or ordering in DPPC, but it is likely due to collective effects of local water ordering in the DPPC/Chol lipid system. In contrast, although the DOPC bilayer system upheld the same trend as seen with DPPC, Chol causes comparatively less changes to the bilayer-internal hydration dynamics in DOPC. These findings suggest that Chol has a greater affinity to DPPC than to DOPC in the binary lipid systems,[36,41] in a way that promotes a more efficient packing of the DPPC membrane to impede rapidly diffusing water across the lipid bilayer. Interestingly, the τ/τ_{bulk} and k_σ values found for the bilayer-internal water in the DOPC/DPPC/Chol system is intermediate of that found with pure DOPC or DPPC lipid membrane systems in the presence of 30 mol.% Chol. However, the starkest contrast is found for k_{low} that shows an extremely low value for the binary DOPC/DPPC in the absence of Chol (lower than in pure DOPC or DPPC bilayers, Fig. 2(c)). When 30 mol.% Chol is added to the DOPC/DPPC mixture, k_{low} dramatically increases to 65% and reaches a similar value as in DOPC or DPPC bilayers with 30 mol.% Chol embedded. This finding implies that the effect of Chol in recruiting bound water population is more significant in the heterogeneous ternary lipid environments than in the homogeneous binary mixture.[46]

C. Hydration dynamics and lipid ordering on the lipid membrane surface of liposomes

We used lipid vesicles with nitroxide radicals (TEMPO-PC) positioned off the polar headgroups of the lipid bilayer to monitor how Chol influences hydration dynamics and lipid ordering on the surface of lipid bilayers. Fig. 3(a) presents τ/τ_{bulk} for surface hydration water in the DOPC, DPPC, and DOPC/DPPC systems in the absence and presence of 30 mol.% Chol. These data show that τ/τ_{bulk} for DOPC surface water diffusion decreases from 5.9 ± 0.1 without Chol to 5.2 ± 0.1 in the presence of 30 mol.% Chol—although the effect is certainly smaller than the difference seen for diffusivity of bilayer-internal water. Notably, the Chol effect on the trend of change for bilayer-internal and surface water diffusion is opposite. Additionally, both pure DPPC and mixed DOPC/DPPC lipid systems show a more significant reduction in τ/τ_{bulk} upon adding 30 mol.% Chol—a decrease from 6.9 ± 0.1 to 5.3 ± 0.2 for DPPC and from 8.4 ± 0.2 to 6.8 ± 0.3 for DOPC/DPPC systems. Similar to what has been observed for bilayer-internal water within Chol-rich membranes, k_σ and k_{low} for surface water are anti-correlated with each other, but their values only moderately change in a

consistent manner upon incorporating 30 mol.% Chol into three systems (Figs. 3(b) and 3(c)). Specifically, incorporating 30 mol.% Chol into DPPC and DOPC/DPPC lipid bilayers leads to a 20% increase in k_σ and a 10% decrease in k_{low} for surface water dynamics, while in pure DOPC bilayers the extent of change of the k_σ and k_{low} values are comparable (∼10%). The data again support the view that Chol more strongly interacts with DPPC to alter the lipid organization or domain size that, in turn, affects the lipid headgroup ordering and surface hydration dynamics. Interestingly, the addition of 30 mol.% Chol makes the lipid headgroups of DPPC more disordered and loosely packed than that of the DOPC bilayers (Fig. 3(d)). In fact, such increased lipid headgroup dynamics on the surface of Chol-rich membranes has been previously reported by ^{31}P NMR[25–28] and ^{2}H NMR.[29]

Taken together, our data in Fig. 3 clearly exhibit that Chol decreases the ordering and packing of the lipid headgroups, concurrently increasing the surface hydration dynamics near the lipid membrane surface. The increased surface hydration dynamics in DOPC, DPPC, and DOPC/DPPC systems with 30% Chol addition, as seen with decreased τ/τ_{bulk} and concurrently increased k_σ and decreased k_{low}, has never been experimentally observed before, nor theoretically predicted by any prior study.

To understand the effect of Chol on the local hydration dynamics and lipid ordering closer to the Chol surface, i.e., slightly below the lipid phosphates, we incorporated 3 mol.% CSL spin probe to replace a fraction of the Chol in the DOPC/DPPC/Chol system. As expected, the nitroxide radical of CSL attached to the rigid sterol group shows a rigid-limit EPR spectrum,[91] as shown in Fig. 1(b). Although the motion of nitroxide moiety of TEMPO-PC is also somewhat restricted by electrostatic interactions with other neighboring headgroups, it can still freely rotate on the membrane surface given the flexible tether connecting the nitroxide moiety to PC (unlike in CSL), yielding an overall lower order parameter than that of the CSL-attached radical probe.[20] Interestingly, the measured τ/τ_{bulk} value of a CSL spin label in the DOPC/DPPC/Chol system is 7.3 ± 0.7, which is the same within error as τ/τ_{bulk} measured with TEMPO-PC of the same ternary lipid system displaying 6.8 ± 0.3. This result suggests that the local hydration dynamics is altered over a significant range of thickness, from 5 to 10 Å above to slightly below the lipid headgroups in DOPC/DPPC/Chol bilayers, presenting a faster water diffusivity compared to on Chol-depleted DOPC/DPPC surfaces. The region below the lipid phosphate of DOPC/DPPC/Chol, as probed by CSL, concurrently finds a much stronger contribution from bound water according to high k_{low} values (Figs. 3(b) and 3(c)). The concurrently high population of bound water together with rapidly diffusing surface water located below phosphate group is a curious observation in the DOPC/DPPC/Chol systems that require a more systematic investigation, as presented in Sec. IV.

D. Hydration dynamics and lipid ordering of the DOPC/DPPC/cholesterol ternary system

Given the distinct observation on surface hydration dynamics made in DOPC/DPPC/Chol systems at 30 mol.% Chol, we present a systematic study on the effect of Chol in the ternary system in the range of 0–50 mol.% Chol concentration. The ODNP parameters in DOPC/DPPC/Chol are listed in Tables S2 and S3 of the supplementary material.[80] Fig. 4(a) presents the retardation factor τ/τ_{bulk} of local water near the bilayer surface and within the bilayers of the ternary mixtures at variable Chol concentrations, along with the indication for the corresponding lipid phases. A DOPC/DPPC mixture is initially in a coexisting $l_d + g$ phase. Upon addition of 10–20 mol.% Chol, a third l_o phase appears.[31–36] Increasing the Chol concentration further (20–30 mol.%) results in the disappearance of the g phase, while the lipid mixture adopts a complete l_o phase at >30 mol.% Chol.[31–33] We observe that, regardless of the different lipid phases present or absent, as Chol concentrations increase from 0 to 50 mol.%, the τ/τ_{bulk} values for bilayer-internal water steadily and significantly increase from 10.5 to 35.3 (Fig. 4(a)), accompanied by a dramatic increase in order parameter S of the hydrocarbon chains within lipid bilayers, as probed by 16DSA (Fig. 4(d)). Not surprisingly, the trends of τ/τ_{bulk} and S are not linearly correlated with the Chol concentration. At low Chol concentration between 0 and 15 mol.%, both τ/τ_{bulk} and S values within the lipid bilayers only modestly change by about 10%–20%. At an intermediate Chol concentration between 15 and 30 mol.%, where a phase transition from a coexisting $l_d + l_o + g$ phase to a $l_d + l_o$ phase occurs, a significant retardation of τ/τ_{bulk} (50%) in bilayer-internal hydration dynamics is observed, originating from moderately decreasing k_σ (Fig. 4(b)) and dramatically increasing k_{low} (Fig. 4(c)). The transition from 30 mol.% to 50 mol.% Chol is accompanied by an even more dramatic reduction in τ/τ_{bulk} (63%), accompanying the disappearance of the l_d phase. Notably, the increase in k_{low} for bilayer-internal water (Fig. 4(c)) is the dominant change with increasing Chol concentration across a wide range of lipid phases, while k_σ only gradually decreases with increasing Chol concentration (Fig. 4(b)). This finding allows us to conclude that it is the increasing population of bound water that plays the major role in retarding the bilayer-internal hydration dynamics in the Chol-containing ternary lipid mixtures. In fact, the dramatic increase in bound water population observed within the bilayers provide strong evidence for the emergence of segregated phases as suggested in the literature,[46,51] in which bound water is contributing to, or at the very least is intimately built into, the tighter lipid packing found in the newly forming l_o phases. In the ternary mixture contained 50 mol.% Chol that is thought to be in a pure l_o phase, the effects of bound bilayer-internal water and tight lipid packing peak at maximal amplitudes, as signified by minimal k_σ, maximal k_{low}, and maximal S value. These results support the hypothesis that in the new equilibrium l_o phase, the flat sterol structure of Chol could efficiently rigidify the fatty acyl chains, thereby impose a conformational ordering of the acyl chains.[38]

Unexpectedly, as discussed in Sec. III C, hydration dynamics on the surface of lipid bilayers clearly increases with increasing Chol content, whose effect is present for all lipid mixtures studied. This effect is most significant in the ternary lipid systems and follows the opposite trend of the bilayer-internal hydration dynamics. As shown in Fig. 4(a), the

surface hydration dynamics increases with increasing Chol concentration, while the lipid headgroups become disordered (Fig. 4(c)). The τ/τ_{bulk} values for surface water undergo a relatively large change from 6.8 ± 0.3 to 5.9 ± 0.5 from 30 to 50 mol.% Chol in the ternary lipid mixture. Increasing k_σ and decreasing k_{low} values as a function of Chol concentration suggest that more rapidly diffusing water and less bound water are hydrating the surface of Chol-rich lipid systems (Figs. 4(b) and 4(c)). The tight lipid tail packing and loose headgroup packing, concurrently observed with a decrease in bilayer-internal hydration dynamics and an increase in surface hydration dynamics, with the most dramatic effect seen at 30–50 mol.% Chol, represent a profound effect of Chol on membrane biophysics. Given that Chol in plasma membranes are found at 30–40 mol.%, the physical properties identified here are likely relevant in unraveling functional effects of Chol on biological lipid membranes and membrane protein systems.

IV. DISCUSSION

The functional role of Chol in biological membranes has been postulated in numerous studies. It has been suggested that biological events, such as protein docking, are strongly influenced by Chol-enriched domains in lipid bilayers.[3] For example, the enzymatic activity of membrane-bound enzyme enhances under Chol-rich conditions, where lipid-raft domains present.[17,18] In this study, we observed enhanced surface water diffusivity in model lipid membrane systems at biologically relevant Chol concentrations, concurrently with dramatically reduced bilayer-internal water diffusion and increased lipid ordering. We postulate that the modulation of hydration dynamics in Chol-containing lipid bilayers could be a key element to influence lipid membrane functions.

It is more obvious how the modulation of local hydration dynamics may simply reflect on changes in lipid membrane structure and stability; however, it is less clear how hydration dynamics can play an active role in modulating biological processes. One possible scenario is that surface hydration dynamics could be favorable towards biomolecular binding events when repulsive interaction at the interface is lowered as a result of weakened hydrogen bonds or lowered electrostatic interactions. This effect would be reflected in faster diffusion of freely moving surface water signified by higher k_σ values. When bound water accumulates at the interface where binding occurs, its release offers entropic gain, and thus thermodynamically favors protein binding to the lipid membrane surface. Although no rigorous cause-and-effect conclusion can be drawn, an increased translational diffusivity of freely moving water on the surface of Chol-containing lipid mixtures is consistently observed, implying that lowered activation energy for water diffusion and lowered repulsive barrier for constituent approach to the surfaces of Chol-containing lipid membranes. Interestingly, the population of bound water is only modest (rather slightly decreasing) at lipid membrane surfaces, but dramatically increases below the phosphate groups, as measured by CSL, as well as in the bilayer interior, as measured by 16DSA. The CSL label is likely quite exposed to water at the lipid-water interface, albeit closer to the membrane bilayer compared to the TEMPO-PC label. Concurrently, the order parameter S for the hydrocarbon region measured from EPR spectra at 30 and 50 mol.% Chol significantly increases, indicating that the motional freedom of lipid acyl chains is dramatically decreased when Chol is embedded. This finding is consistent with the well-accepted property of retarded permeability of water and small solutes across lipid bilayers in the presence of Chol.[20,42–45] Overall, the differentially changing hydration dynamics within the bilayer and on the surface of lipid membranes clearly showcases the dramatic impact of Chol on the structural organization of lipid properties. The capability of ODNP relaxometry that can sensitively and selectively detect local hydration dynamics within 5–10 Å of spin labels embedded in PC bilayers with varying Chol contents allows for unprecedented accounts of physical effects of Chol on lipid membranes, which could serve as starting point of delineating the mechanism of Chol function. We note that the spin labels tethered on lipids only minimally affect the surface hydration dynamics measured, but the systematic experimental outcome presented herein should be convincing for such perturbation effects to be negligible, if they exist. Generally, more subtle changes in hydration dynamics as observed with ions or small molecules near spin probes tethered to molecular surfaces are more difficult to unambiguously attribute to changes in surface properties, in which case reference measurements using freely dissolved spin labels in the same solvent as the immersed surface are needed.[7] However, dramatic effects on local water properties as seen in lipid bilayers with increasing Chol content can be relatively noninvasively read out using spin labeled lipids. It should be emphasized that we cannot exclude the possibility that Chol may have a different affinity to different phospholipids vs. spin-labeled lipids or surfactants, so that a complete averaging of the water protons may not necessarily take place in these phase-segregated systems. Thus, the parameters extracted from ODNP and cw EPR lineshapes may not strictly represent an average value in this regime, but certainly reports on qualitatively valid trends.

Even though the moderate decreases in τ/τ_{bulk} on the surface water have to be interpreted cautiously, the qualitative trends of increasing k_σ and decreasing k_{low} of surface water as a function of Chol concentration unambiguously confirms that increasing Chol content enhances water mobility on lipid membrane surfaces. This is interesting in light of previous EPR studies demonstrated that the surface of the Chol-rich bilayers is more hydrated than Chol-depleted bilayers.[85,92,93] Moreover, an early neutron reflectivity study observed that the roughness of DPPC bilayer surfaces increases with Chol content, likely resulting from Chol interfering with the packing of DPPC molecules.[94] Therefore, a high Chol content could generate more packing defects on membrane surfaces, distorting the comparably smooth and sealed surface of Chol-less bilayers.[95] The physical roughness of the membrane surface may perturb or weaken the stability of hydrogen-bond network of the surrounding water associated with the lipid membrane surface,[57,96] thereby enhancing surface water diffusivity. Furthermore, we believe that the decreased ordering of lipid headgroups should not directly cause increased surface hydration dynamics, because their overall dynamics are

occurring at very different timescales (tens of ns for EPR vs. hundreds of ps for ODNP).

Hydration water is important in mediating enzymatic activity,[17,18] whose role may be framed in a unified model for protein dynamics.[96] This model suggests that the fluctuation in surface water mediates motional and conformational changes of the protein and ligand migration, thereby influencing biological functions. While such models need firm experimental verification that has not occurred to date, ODNP data demonstrate increased surface water diffusivity in DOPC/DPPC/Chol systems with these effects peaking under lipid raft-forming conditions. We may postulate that increased enzymatic activity of membrane proteins in Chol-rich lipid membranes could be facilitated by increased surface hydration dynamics under raft-forming conditions. The dramatically decreased water dynamics and increased lipid ordering within the hydrocarbon region of the Chol-containing bilayers would possibly increase the potential of active ion- or water-channel proteins by decreasing passive leakage of ions and water through the lipid bilayer, as well as generally increase membrane protein integrity and lipid membrane stability. Further investigation is needed to prove these hypotheses.

V. CONCLUSION

In this study, the effect of Chol on the local hydration dynamics of lipid bilayer systems, either on the surface or within the hydrophobic core of lipid bilayers, is systematically measured by ODNP and cw EPR. At higher Chol concentrations, DOPC/DPPC/Chol mixtures display increased surface water diffusivity and significantly reduced water diffusivity within the hydrophobic core of lipid bilayers. Additionally, bound water populations significantly increase at the lipid-water interface and hydrophobic core, concurrent with loosing packing of lipid headgroups and dramatically increased ordering of the lipid acyl chains. This work clearly demonstrates that the dynamics of hydration water interacting with Chol-containing lipid vesicles is differentially affected at specific spatial regions or sites. The functional role of Chol-rich lipid domains or lipid rafts may hinge on significantly enhanced surface water diffusivity that should lower the energy barrier for proteins, ligands or other biological constituents to approach to lipid membrane surfaces. The Chol could increase membrane protein integrity and stability by tightly hugging the membrane protein with lipid. Chol may be possibly entropically favoring protein binding on lipid raft surfaces by offering the opportunity to release bound water population from the interface. Although further investigations are needed to support the above hypothesis, this study serves as a starting point to understand the role of Chol in the cell membrane, which regulated and harnessed numerous biological functions within the Chol-rich nano-patches.

VI. MATERIALS AND METHODS

A. Materials

Phospholipids 1,2-dioleoyl-*sn*-glycero-3-phosphocholine (DOPC), 1,2-dipalmitoyl-*sn*-glycero-3-phosphocholine (DPPC), and TEMPO-PC (1,2-dioleoyl-*sn*-glycero-3-phospho(tempo)choline) were purchased from Avanti Polar Lipids (Alabaster, AL) and used without further purification. Cholesterol (Chol), 16-doxyl-stearic acid (16DSA), and 3β-doxyl-5α-cholestane (CSL) were purchased from Sigma-Aldrich (St. Louis, MO) and used without further purification.

B. Lipid vesicle preparation

The lipids and cholesterol were dissolved in a solvent composed of chloroform:methanol (9:1, v:v). Lipids were dried under nitrogen atmosphere for 20 min and under vacuum overnight. Lipids were hydrated with Millipore water and a lipid concentration of 30 mM is used. Hydrated lipids were vortexed at low speed for at least 1 h above the transition temperature. A concentration of 0.7 mM is used for both the TEMPO-PC and 16DSA spin labels (2 mol.% of lipid content) and 0.95 mM (3 mol.%) for CSL. Large unilamellar vesicles (LUV) were prepared by extrusion through a 200 nm membrane using a mini-extruder from Avanti Polar Liquids (Alabaster, AL). Vesicles were prepared one day before measurements and stored at 4 °C before measurements. Dynamic Light Scattering using a Nano-Series Zetasizer (Nano-ZS ZEN3600; Malvern Instruments, Worcestershire, United Kingdom) showed uniform sized vesicles.

C. EPR and ODNP measurements

cw EPR spectra were acquired on a Bruker EMX X-band spectrometer at room temperature. The EPR spectra were acquired using a standard cylindrical TE_{011} resonator (ER 4119HS-LC, Bruker, Billerica, MA) at room temperature. The conventional EPR spectra were acquired using 20 mW microwave power and 100 kHz field modulation with an amplitude of 2 Gauss. The field scan was 10 mT with field centre of 348.5 mT. 1024 data points were recorded with a time constant of 20 ms and the scan rate was 11.4 mT/min.

Both ODNP and EPR measurements were performed at room temperature, T = 25 °C. For ODNP measurements, lipid samples were loaded into a 0.6 mm i.d. 0.84 mm o.d. quartz capillary and sealed both ends with capillary wax. The capillary was loaded into a homebuilt NMR probe and placed inside a Bruker TE_{102} X-band cavity. EPR spectra were acquired to determine the center field with a Bruker EMX spectrometer. ^{1}H NMR measurements were performed using a Bruker Avance 300 NMR spectrometer. The magnetic field for ODNP experiments was 0.35 T. During the ODNP measurements, the samples were continuously irradiated at the EPR frequency by a home-built 8–10 GHz microwave amplifier. T_1 measurements were conducted by a typical inversion-recovery pulse sequence in a 0.35 T superconductive magnet using a Kea spectrometer (Magritek, Wellington, New Zealand). Cooling air was flowed over the sample during the measurement, and microwave powers were kept lower than maximum to avoid sample heating. Error bar represents the standard deviation, which was obtained from two to five repeat measurements.

ACKNOWLEDGMENTS

We acknowledge support by the 2011 NIH Director New Innovator Awards. This work made use of the Materials Research Laboratory (MRL) Central Facilities supported by National Science Foundation (NSF) through MRSEC (DMR 1121053). The MRL is a member of the NSF-funded Materials Research Facilities Network (http://www.mrfn.org). This work was partially funded by the UCSB CISEI program through the NSF Research Experiences for Undergraduates (NSF DMR 0843934).

[1] J. N. Israelachvili, D. J. Mitchell, and B. W. Ninham, J. Chem. Soc. Faraday Trans. 2 **72**, 1525 (1976).
[2] H. X. Zhou and T. A. Cross, Annu. Rev. Biophys. **42**, 361 (2013).
[3] R. Santos, J. Hritz, and C. Oostenbrink, J. Chem. Inf. Model **50**, 146 (2010).
[4] T. M. Raschke, Curr. Opin. Struct. Biol. **16**, 152 (2006).
[5] R. Kausik and S. Han, J. Am. Chem. Soc. **131**, 18254 (2009).
[6] C. Y. Cheng *et al.*, Proc. Natl. Acad. Sci. U.S.A. **110**, 16838 (2013).
[7] J. Song *et al.*, J. Am. Chem. Soc. **136**, 2642 (2014).
[8] P. W. Fenimore *et al.*, Proc. Natl. Acad. Sci. U.S.A. **99**, 16047 (2002).
[9] S. Roy and B. Bagchi, J. Phys. Chem. B **116**, 2958 (2012).
[10] O. S. Andersen, Nat. Chem. Biol. **9**, 667 (2013).
[11] D. Lingwood and K. Simons, Science **327**, 46 (2010).
[12] O. S. Andersen and R. E. Koeppe, Annu. Rev. Biophys. Biomol. Struct. **36**, 107 (2007).
[13] J. Gatfield and J. Pieters, Science **288**, 1647 (2000).
[14] F. R. Maxfield and I. Tabas, Nature (London) **438**, 612 (2005).
[15] M. B. Jackson, Proc. Natl. Acad. Sci. U.S.A. **86**, 2199 (1989).
[16] C. Ho and C. D. Stubbs, Biophys. J. **63**, 897 (1992).
[17] C. P. Sotomayor *et al.*, Biochemistry **39**, 10928 (2000).
[18] F. J. Cuevas, D. M. Jameson, and C. P. Sotomayor, Biochemistry **45**, 13855 (2006).
[19] P. L. Yeagle, Biochimie **73**, 1303 (1991).
[20] W. K. Subczynski *et al.*, Biochemistry **33**, 7670 (1994).
[21] B. Dzikovski, D. Tipikin, and J. Freed, J. Phys. Chem. B **116**, 6694 (2012).
[22] M. Ge and J. H. Freed, Biophys. J. **85**, 4023 (2003).
[23] M. Ge *et al.*, Biophys. J. **77**, 925 (1999).
[24] J. P. Barnes and J. H. Freed, Biophys. J. **75**, 2532 (1998).
[25] A. L. Costello and T. M. Alam, Chem. Phys. Lipid. **163**, 506 (2010).
[26] A. L. Costello and T. M. Alam, Biochim. Biophys. Acta **1778**, 97 (2008).
[27] G. P. Holland, S. K. McIntyre, and T. M. Alam, Biophys. J. **90**, 4248 (2006).
[28] T. Pott, J. C. Maillet, and E. J. Dufourc, Biophys. J. **69**, 1897 (1995).
[29] M. F. Brown and J. Seelig, Biochemistry **17**, 381 (1978).
[30] M. Mihailescu *et al.*, J. Membr. Biol. **239**, 63 (2011).
[31] J. Juhasz, F. J. Sharom, and J. H. Davis, Biochim. Biophys. Acta **1788**, 2541 (2009).
[32] J. H. Davis, J. J. Clair, and J. Juhasz, Biophys. J. **96**, 521 (2009).
[33] S. L. Veatch and S. L. Keller, Biophys. J. **85**, 3074 (2003).
[34] B. L. Stottrup, D. S. Stevens, and S. L. Keller, Biophys. J. **88**, 269 (2005).
[35] S. L. Veatch and S. L. Keller, Biochim. Biophys. Acta. **1746**, 172 (2005).
[36] N. Kahya *et al.*, J. Struct. Biol. **147**, 77 (2004).
[37] W. K. Subczynski *et al.*, Biophys. J. **92**, 1573 (2007).
[38] D. Marsh and I. C. Smith, Biochim. Biophys. Acta **298**, 133 (1973).
[39] A. J. Costa-Filho, Y. Shimoyama, and J. H. Freed, Biophys. J. **84**, 2619 (2003).
[40] M. J. Swamy *et al.*, Biophys. J. **90**, 4452 (2006).
[41] F. de Meyer and B. Smit, Proc. Natl. Acad. Sci. U.S.A. **106**, 3654 (2009).
[42] J. C. Mathai *et al.*, J. Gen. Physiol. **131**, 69 (2008).
[43] C. Y. Cheng, O. J. G. M. Goor, and S. Han, Anal. Chem. **84**(21), 8936 (2012).
[44] A. Carruthers and D. L. Melchior, Biochemistry **22**, 5797 (1983).
[45] R. Fettiplace and D. A. Haydon, Physiol. Rev. **60**, 510 (1980).
[46] G. W. Feigenson, Biochim. Biophys. Acta **1788**, 47 (2009).
[47] G. W. Feigenson, Annu. Rev. Biophys. Biomol. Struct. **36**, 63 (2007).
[48] C. L. Armstrong *et al.*, PloS ONE **8**, e66162 (2013).
[49] K. Suga and H. Umakoshi, Langmuir **29**, 4830 (2013).
[50] M. R. Vist and J. H. Davis, Biochemistry **29**, 451 (1990).
[51] A. C. Brown and S. P. Wrenn, Langmuir **29**, 9832 (2013).
[52] S. Ebbinghaus *et al.*, Proc. Natl. Acad. Sci. U.S.A. **104**, 20749 (2007).
[53] N. V. Nucci, M. S. Pometun, and A. J. Wand, J. Am. Chem. Soc. **133**, 12326 (2011).
[54] B. Halle, Philos. Trans. R. Soc. Lond. Ser. B **359**, 1207 (2004).
[55] L. Y. Zhang *et al.*, J. Am. Chem. Soc. **131**, 10677 (2009).
[56] M. Tarek and D. J. Tobias, Biophys. J. **79**, 3244 (2000).
[57] D. Russo, G. Hura, and T. Head-Gordon, Biophys. J. **86**, 1852 (2004).
[58] C. Y. Lee, J. A. Mccammon, and P. J. Rossky, J. Chem. Phys. **80**, 4448 (1984).
[59] B. D. Armstrong and S. Han, J. Chem. Phys. **127**, 104508 (2007).
[60] B. D. Armstrong and S. Han, J. Am. Chem. Soc. **131**, 4641 (2009).
[61] J. M. Franck *et al.*, Prog. Nucl. Magn. Reson. Spectrosc. **74**, 33 (2013).
[62] K. H. Hausser and D. Stehlik, Adv. Magn. Reson. **3**, 79 (1968).
[63] B. H. Robinson, D. A. Haas, and C. Mailer, Science **263**, 490 (1994).
[64] C. Y. Cheng and S. Han, Annu. Rev. Phys. Chem. **64**, 507 (2013).
[65] C. Y. Cheng *et al.*, J. Magn. Reson. **215**, 115 (2012).
[66] C. Y. Cheng *et al.*, Biomacromolecules **13**, 2624 (2012).
[67] R. Kausik and S. Han, Phys. Chem. Chem. Phys. **13**, 7732 (2011).
[68] B. D. Armstrong *et al.*, J. Am. Chem. Soc. **133**, 5987 (2011).
[69] S. Hussain, J. M. Franck, and S. Han, Angew. Chem.-Int. Edit. **52**, 1953 (2013).
[70] J. M. Franck, J. A. Scott, and S. Han, J. Am. Chem. Soc. **135**, 4175 (2013).
[71] L. P. Hwang and J. H. Freed, J. Chem. Phys. **63**, 4017 (1975).
[72] M. W. Hodges *et al.*, Biophys. J. **73**, 2575 (1997).
[73] J. Kowalewski *et al.*, Prog. Nucl. Magn. Reson. Spectrosc. **17**, 141 (1985).
[74] H. F. Bennett *et al.*, Magn. Reson. Med. **4**, 93 (1987).
[75] C. F. Polnaszek and R. G. Bryant, J. Chem. Phys. **81**, 4038 (1984).
[76] H. Jansson *et al.*, J. Chem. Phys. **130**, 205101 (2009).
[77] J. L. MacCallum and D. P. Tieleman, Trends Biochem. Sci. **36**, 653 (2011).
[78] D. J. Tobias, K. C. Tu, and M. L. Klein, Curr. Opin. Colloid Interface Sci. **2**, 15 (1997).
[79] M. Gutman and E. Nachliel, Biochim. Biophys. Acta-Bioenerg. **1231**, 123 (1995).
[80] See supplementary material at http://dx.doi.org/10.1063/1.4897539 for details of the ODNP parameters.
[81] W. L. Hubbell and H. M. McConnell, J. Am. Chem. Soc. **93**, 314 (1971).
[82] Z. T. Farahbakhsh, C. Altenbach, and W. L. Hubbell, Photochem. Photobiol. **56**, 1019 (1992).
[83] J. P. Barnes and J. H. Freed, Rev. Sci. Instrum. **68**, 2838 (1997).
[84] H. Fukuda *et al.*, Langmuir **17**, 4223 (2001).
[85] D. Marsh, Proc. Natl. Acad. Sci. U.S.A. **98**, 7777 (2001).
[86] P. Barre and D. Eliezer, J. Mol. Biol. **362**, 312 (2006).
[87] C. Altenbach *et al.*, Proc. Natl. Acad. Sci. U.S.A. **91**, 1667 (1994).
[88] A. A. Musse, J. M. Boggs, and G. Harauz, Proc. Natl. Acad. Sci. U.S.A. **103**, 4422 (2006).
[89] T. Lazrak *et al.*, Biochim. Biophys. Acta **903**, 132 (1987).
[90] L. Mainali *et al.*, J. Magn. Reson. **212**, 418 (2011).
[91] A. Kusumi and M. Pasenkiewicz-Gierula, Biochemistry **27**, 4407 (1988).
[92] D. Marsh, Eur. Biophys. J. **31**, 559 (2002).
[93] N. Manukovsky *et al.*, Mol. Phys. **111**, 2887 (2013).
[94] B. Stidder, G. Fragneto, and S. J. Roser, Langmuir **21**, 9187 (2005).
[95] M. R. Ali, K. H. Cheng, and J. Huang, Proc. Natl. Acad. Sci. U.S.A. **104**, 5372 (2007).
[96] H. Frauenfelder *et al.*, Proc. Natl. Acad. Sci. U.S.A. **106**, 5129 (2009).